CHAPTER 4 AN IMPINGEMENT FLAME OF SPMB AND CB

From a fundamental knowledge of the SPMB in chapter 3, we understand a behavior and limitation of the SPMB but the results of them base on a free flame phenomenon that does not reflect a real application. So this chapter presents a performance of an impinging flame of the SPMB such as thermal efficiency and emission characteristics which test nearly real application conditions in the SMEs. Moreover, the results of the SPMB compared with the CB and the thermal efficiency of both burners use to calculated an energy saving.

4.1 Experiment setup

Details of the SPMB for thermal performance test in this section are well documented in chapter 3, thus only a brief description is given here. Figure 4.1 shows a schematic diagram of the experimental setup for an impingement flame of the SPMB, which consist mainly composed of four parts: a mixing tube (5), a mixing chamber (6), a perforated stainless steel plate (7) and a packed bed (8). The SPMB was placed on adjustable base (17). Flame from burner was impinged on a cylindrical vessel containing water (16) with a flat bottom surface diameter of 920 mm and 800 mm height, which is made from a stainless steel. A liquefied petroleum gas (LPG) (1) was selected as a fuel in the experiment because of its widespread use in Thailand's SMEs. The LPG contains 30% (by volume) of propane (C_3H_8) and 70% (by volume) of butane (C_4H_{10}) with a low heating value of about 106.5 MJ/m^3 [normal]. It is controlled by a high pressure regulator (2) with calibrated high pressure flow meter (3) and ball valve (4) that is connected with the fuel nozzle having diameter of 1.5 mm. It is lower than a free flame test because the primary aeration is decreased by an increasing of gas fuel nozzle diameter (as shown in figure B.1) and if a small diameter of gas fuel nozzle that provides a low capacity range of firing rate. Thus, the gas fuel nozzle diameter in this test is selected at 1.5 mm because of a suitable of primary aeration and wide range of firing rate (effect of gas fuel nozzle diameter on thermal performance of the SPMB is shown in figures B.7 to B.10). Water temperature was monitored by a K-type sheath thermocouple (10) with a wire diameter of 0.5 mm and located at a quarter of vessel diameter, as shown in figure 4.1. Signal of thermocouple is digitized by a data logger

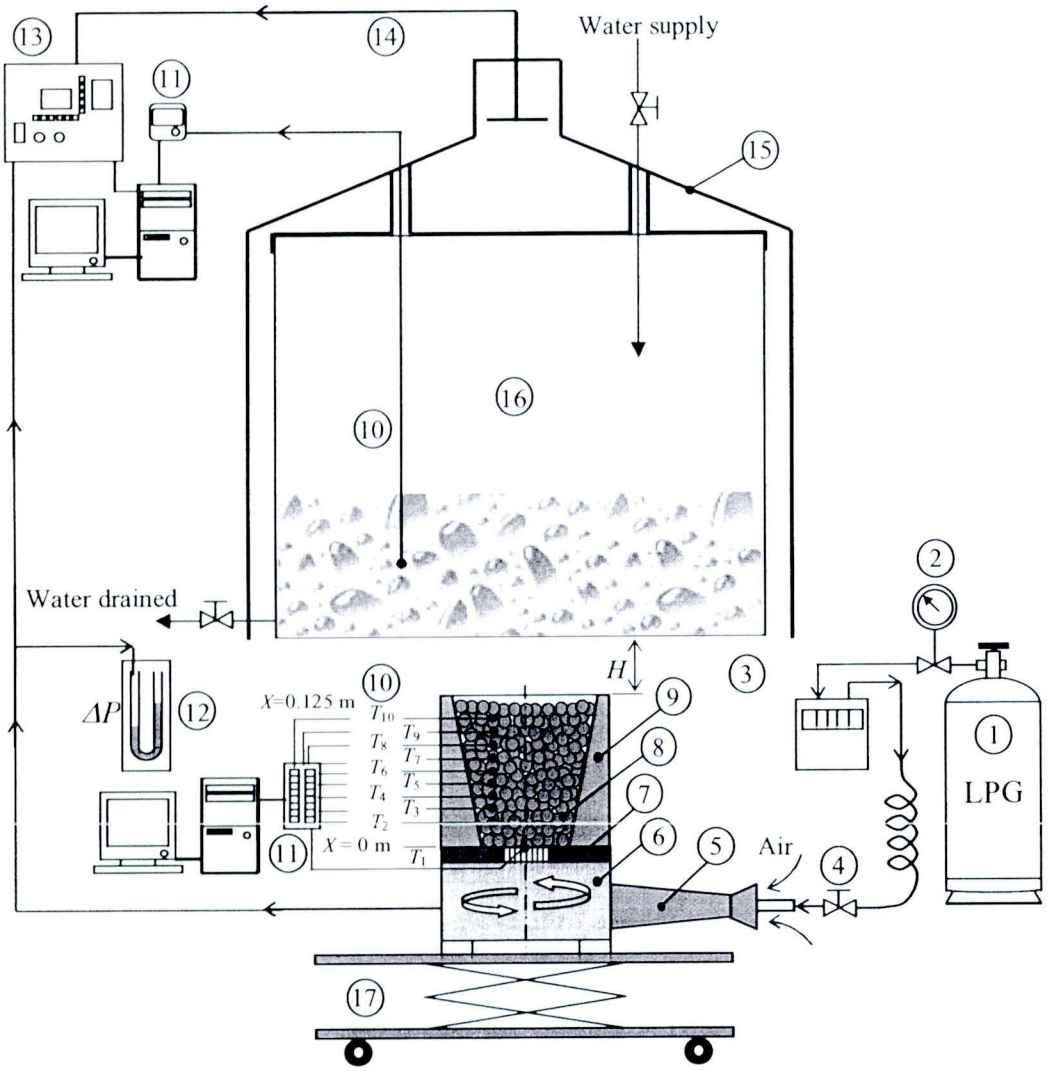

1. Fuel (LPG); 2. Pressure gauge; 3. High pressure gas flow meter; 4. Ball valve & gas fuel nozzle; 5. Mixing tube; 6. Mixing chamber; 7. Perforated stainless steel plate; 8. Packed bed burner; 9. High temperature cement; 10. Thermocouples; 11. Data logger; 12. Water manometer; 13. Exhaust gas analyzer & oxygen sensor; 14. Sampling probe; 15. Hood; 16. Vessel containing water; 17. Adjustable base.

Figure 4.1 Schematic diagram of SPMB's impinging flame experiment setup.

(Testo model 175-T3)(11), and then transmitted to a personal computer. An oxygen (O_2) concentration within the fresh mixture and pressure drop across the packed bed (8) is measured by the oxygen sensor (13) and water manometer (12), respectively. It is sucked at the side wall of mixing chamber (6), with an accuracy of about 0.05%. An uncertainty analysis of O_2 sensor was carried out with the method proposed by Kline and McClintock [41]. The O_2 concentration is used for estimating the primary aeration (*PA*) of the air entrainment into the mixing tube [11] to observe quality of the mixture. A hood (15) for collecting a flue gas was designed and constructed from using European

standards, EN 203-1:1992 [48] and EN 203-2:1995 [49], as a guideline. The vessel is covered by a hood for collecting the exhaust gases separately from the generated water steam, which is vented through the vertical channels integrated into the hood, see detail in Ref. [1]. The exhaust gases are then sampled by a probe (14) connected to an emission analyzer at the hood exit. Emission analysis is carried out by using a portable exhaust gas analyzer (13) (Messtechnik Eheim model Visit 01L). A gas processing system of CO and NO_x is especially tuned for electrochemical sensors, ensuring long-time stability and accuracy of measurement. The measuring range of the analyzer is 0-10,000 ppm for CO and 0-4,000 ppm for NO_x with a measuring accuracy of about ±5 ppm (from the measure value) and a resolution of 1 ppm for both CO and NO_x. All emission measurements in this experiment are those corrected to 0% excess O_2 and dry-basis.

The thermal efficiency and emission tests in this work that were modified from the reference standard [48-49]. There were not operated simultaneously. For thermal efficiency test, the vessel was filled with 100 liters of water at room temperature and the burner with the fixed H was already in steady state (start from hot). Then the water temperature heated up to 90°C, the quantity of LPG from high pressure gas flow meter and the usage time from calibrated digital clock, in which were recorded to calculate the thermal efficiency. After that the emissions data were measured while the burner was continually heated until the temperature of water was raised to 100°C.

Thermal efficiency, η_{th}, is calculated according to the European standards [49]. The η_{th} is defined as the ratio of the sensible heat absorbed by the specified water mass (m_w = 100 kg), to raised its temperature from an initial value $T_{w,i}$ to 90°C, to the combustion heat of the burned LPG, as expressed by Eq. (4.1)

$$\eta_{th} = \frac{m_w c_{p,w} (90 - T_{w,i})}{V_c \times LHV} \times 100\% \tag{4.1}$$

where

$$V_c = V_{mes} \times \frac{p_a + p - p_w}{1013.25} \times \frac{288.15}{273.15 + T_g} \tag{4.2}$$

p_a is pressure of ambient air and p_w is approximated by the saturation pressure of the water vapor at the corresponding measured gas temperature, T_g. The reason for taking p_w into account as shown in Eq. (4.2) comes from the fact that the gas flow meter used in the present study is a wet type. Therefore some of water vapor will contain within

Table 4.1 Experimental conditions for impinging flame.

Parameter	Value	Unit
CL	21, 34 and 44	kW
H	50, 75, 100 and 125	mm

the gas because of vaporization of the water. As a consequence, the measured total gas pressure p has to be corrected by subtracting it with the partial pressure p_w of the water vapor containing within it. Neglecting p_w can cause a reduction in thermal efficiency by about 2% [1].

The thermal efficiencies and emission characteristics of the CB and SPMB were compared experimentally at various firing rate, *CL*, and distance between the burner top and the bottom of the loading vessel, *H*, as shown in the figure 4.1. Details of experimental condition of the CB and the SPMB shows in table 4.1.

4.2 Results of impinging flame of the SPMB

4.2.1 Primary aeration.

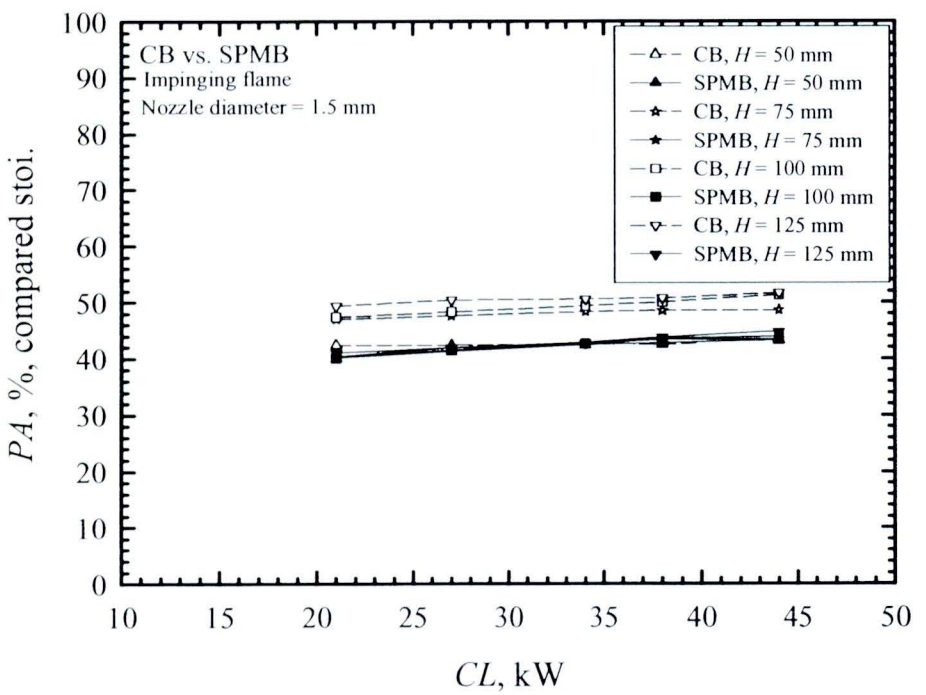

Figure 4.2 Primary aeration of impinging flame.

Figure 4.2 shows comparison of the *PA* between SPMB and CB. The measurement methodology and calculation of *PA* used by Namkhat and Jugjai [11] is applied in this section. Within the range of *CL*, the *PA* of the SPMB and CB are almost linearly increased with *CL* because of a fundamental phenomenon of the self-aspirating burner [42]. But the *PA* of the CB is more than the SPMB due to an increasing of primary air viscosity in the SPMB that is caused by a self-preheating effect from combustion with matrix-stabilized flame [26]. The *PA* of CB increases with *H* because of a decreasing of wall pressure at stagnation point of multiple flame jets [50], leading to a reduction in pressure drop across the mixing chamber when *H* increase. Hence the pressure drop across the mixing chamber has more effects on the *PA* [11]. However the *PA* of SPMB is quietly sense with *H* when compared with the CB due to a strong effect of high velocity of single flame jet from. The measured *PA* of the SPMB is varying from 40 to 45 percent that implies a fuel-rich combustion regime. So the corresponding primary equivalence ratio is ranged from 2.22 to 2.50. This depicts an advantage of combustion with porous medium technology that can be operated with fuel-rich condition.

4.2.2 Emission characteristics

With LPG combustion, the primary pollutants in the flue gas are CO and NO_x [51]. Figure 4.3 and 4.4 show effect of the firing rate *CL* and *H* on CO and NO_x emissions, respectively. Error bars show range or span, which is a difference in maximum and minimum values of the experimental data. The measured values of CO and NO_x do not reflex actual combustion characteristics within the packed bed since the sampling probe is not placed inside the packed bed but it is located at the exit of the exhaust hood. However these measured values of CO and NO_x are adopted in the present study because this agrees with a practical application in which emission measurement must be done at the exit of exhaust hood. All measured emission values are corrected to 0% excess oxygen (0% O_2).

The CO emission level of both burners have a same trend that decrease monotonically as *CL* and/or *H* increased because a more secondary air entrained toward the reaction region to enhance the combustion [52]. However the CO emission of CB is lower than the SPMB because a flame of CB is a multiple-jet flame that easily entrains the secondary air into the reaction zone when compared with a long plume flame from the SPMB [53] , resulting in a more complete combustion in the CB. In addition the *PA* of

CB is higher than the SPMB (see in figure 4.2) that causes a low level of CO in the CB. At $CL > 34$ kW and $H > 75$ mm, the CO emission level of SPMB is lower than the Thai Industrial Standard (T.I.S.) [54], as shown in figure 4.3, that is caused by a sufficient of primary air and more secondary air. At $H = 125$ mm, CO emission of the CB slightly increases with high CL (more than 34 kW). With a short flame of the CB and high H which has a more resident time for dissociation of CO_2 to CO [55] thus an increasing in CO emission at high CL and H of the CB.

Emission level of NO_x is increased with CL and/or H in both burners because of more complete combustion and high flame temperature. A reason of higher NO_x level in CB that has more the PA (see figure 4.2) as a result in complete combustion. The SPMB provides a lower NO_x emission than the CB because a unique characteristic of the porous medium technology that is capable of suppressing the NO_x formation [56-58]. And another reason of low NO_x in the SPMB is a non complete combustion because of a low PA, as shows in figure 4.2. However, the NO_x level increases at high CL and/or H of both burners due to a high temperature (the impingement flame temperature distribution in the packed bed of the SPMB are shown in next section). The values of emissions are shown in table 4.2.

Table 4.2 Emission level of impinging flame of the SPMB.

CL, kW	H, mm	Average CO, ppm at $0\%O_2$		Average NO_x, ppm at $0\%O_2$	
		CB	SPMB	CB	SPMB
21	50	1148	6221	43	10
	75	540	4443	60	12
	100	369	3055	100	14
	125	134	2557	115	19
34	50	1025	3805	44	16
	75	399	2837	63	24
	100	233	2037	103	27
	125	182	1090	109	30
43	50	812	2803	64	27
	75	335	1753	83	37
	100	199	1019	103	53
	125	403	797	112	58

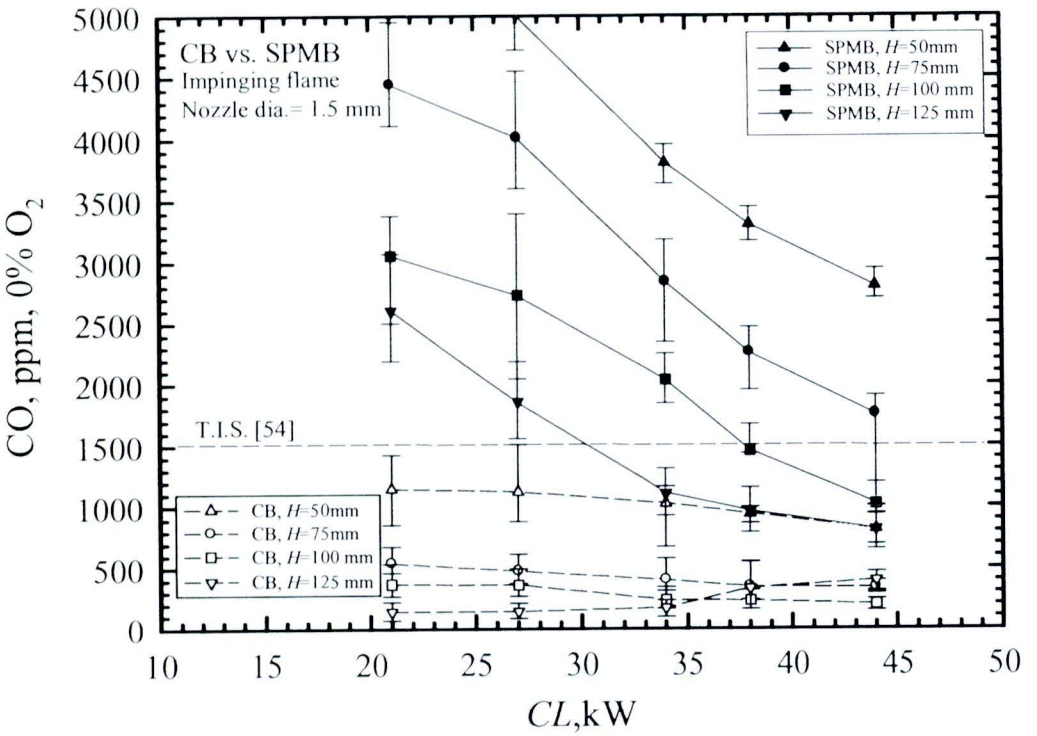

Figure 4.3 CO emissions of impinging flame of the SPMB and CB.

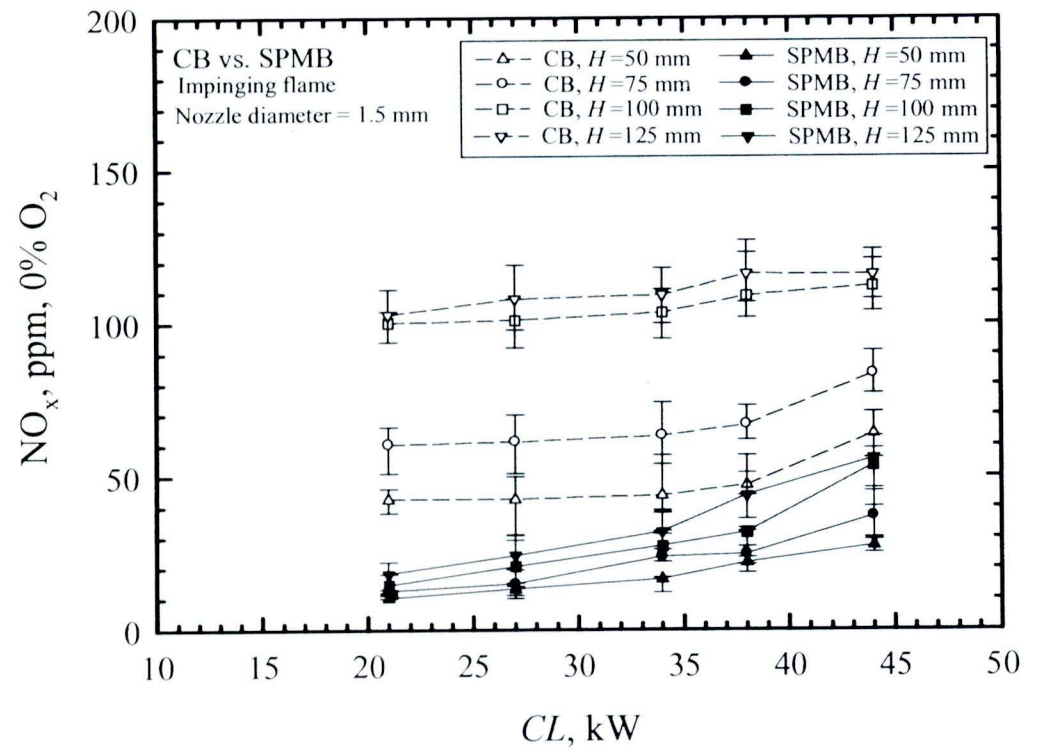

Figure 4.4 NO_x emissions of impinging flame of the SPMB and CB.

4.2.3 Temperature distribution

Figure 4.5 to 4.7 show an effect of H on the temperature profiles along the axis X of the packed bed at CL varying from 21 to 44 kW. All temperature distribution results show that the firing rate CL is considered as a major controlling parameter of the SPMB performance. The trends of temperature profile in the packed bed are similar to the free flame temperature profile in figure 3.7 except at downstream region that there are lower than a free flame case because of heat loss to water load. At constant H, the maximum temperature in the packed bed increases with CL and is almost located at two positions, X = 0.10 m and 0.1125 m, as shown in table 4.3, because of an increasing in heat supply. At CL = 21 kW, H is a dominant parameter on temperature profile. It decreases as H is increased because of a reduction of preheating effect. But this effect not occurs at high firing rate or high flow rate (CL > 21 kW), as shown in figure 4.6 and 4.7. For CL > 21 kW, the upstream temperature is very low because of a high quenching effect from a high velocity of cool mixture and a downstream temperature trend has a similar to a free flame case in the chapter 3 but it is lower than a free flame because a heat is transferred to load and surrounding.

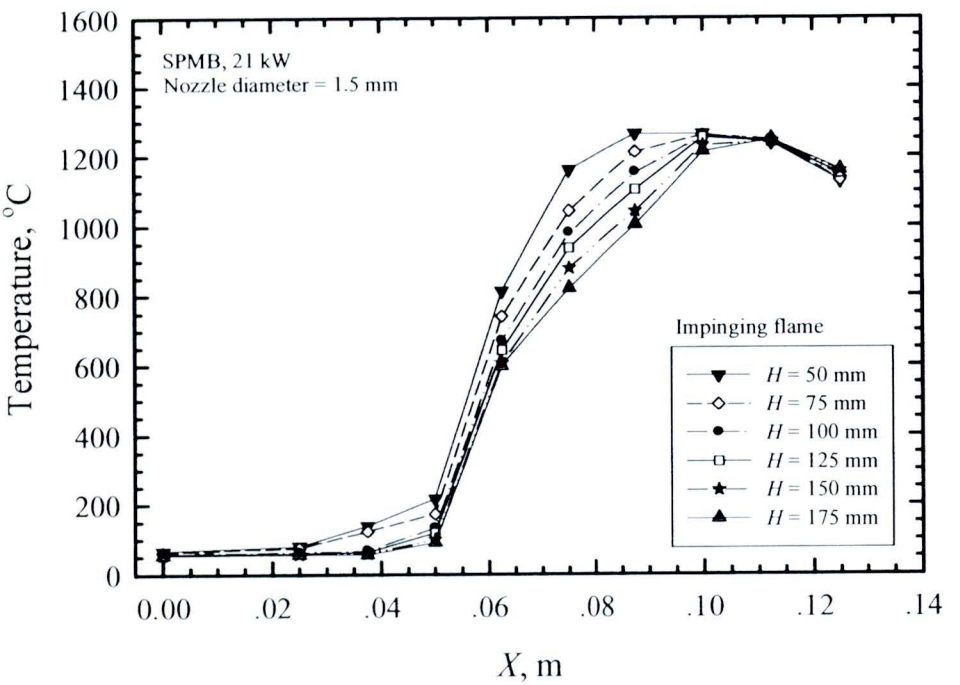

Figure 4.5 Temperature distributions in packed bed of impinging flame at 21 kW.

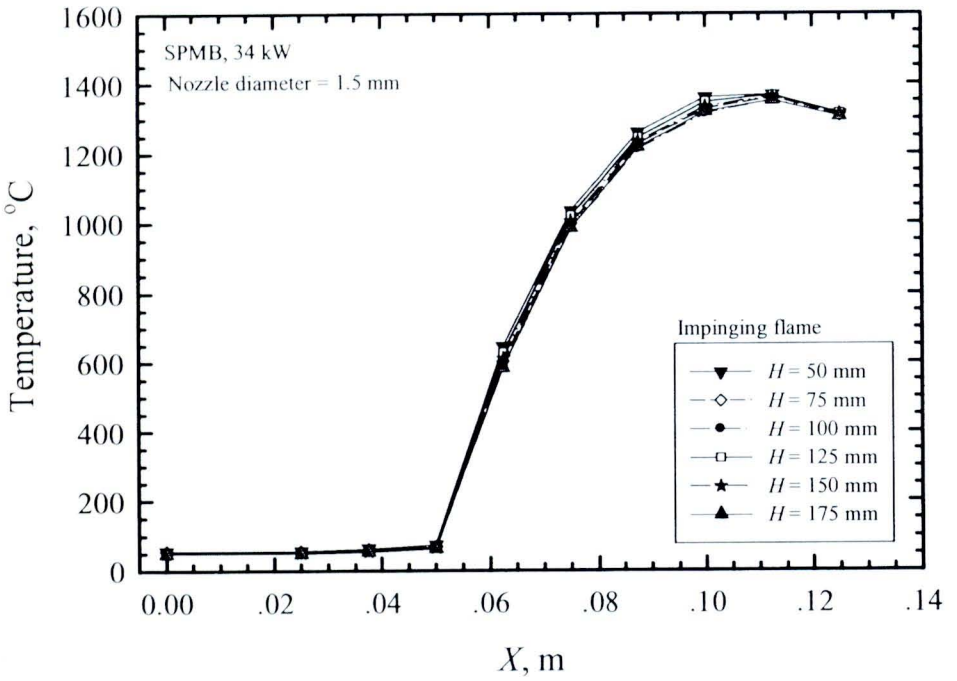

Figure 4.6 Temperature distributions in packed bed of impinging flame at 34 kW.

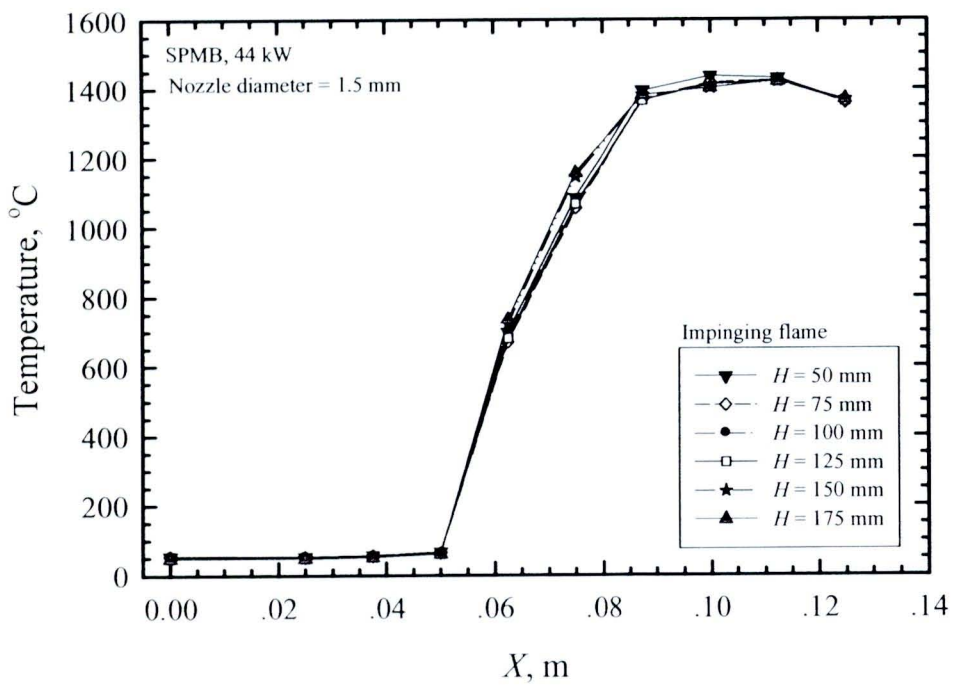

Figure 4.7 Temperature distributions in packed bed of impinging flame at 44 kW.

Table 4.3 Maximum temperature in packed bed of the SPMB.

H, mm	21 kW		34 kW		44 kW	
	T_{max}, °C	Position	T_{max}, °C	Position	T_{max}, °C	Position
50	1,265	T_8	1,367	T_9	1,436	T_8
75	1,260	T_8	1,359	T_9	1,424	T_9
100	1,256	T_8	1,353	T_9	1,423	T_9
125	1,254	T_8	1,366	T_9	1,421	T_9
150	1,242	T_9	1,362	T_9	1,421	T_9
175	1,249	T_9	1,352	T_9	1,421	T_9

The peak temperatures in figures 4.5 to 4.7 imply that a reaction zone in the packed bed. It means that the flame can be stabilized within the packed bed. A location of the peak temperature is settled at T_8 or T_9 which is a suitable position due to a high temperature is near a vessel of load and it causes a high heat transfer rate.

4.2.4 Thermal efficiency

Figure 4.8 shows the comparison of thermal efficiency between the CB and SPMB at various CL and H. As CL increases, the thermal efficiency of both burners decrease monotonically because a high heat loss to surrounding. For increasing in H of both burners, the hottest zone is at some distance away from the bottom of vessel in which the thermal efficiency consequently decreases. This result shows a good agreement with Ref. [5, 59]. For almost conditions, the thermal efficiencies of the SPMB are higher the other burner. Except at $H = 50$ mm and $CL \geq 34$ kW, the thermal efficiency of the CB is higher than one because a flame characteristic of the CB is a multiple-flame jet that has a short flame length. Thus an intense combustion zone can be occurs near the surface of the loading vessel when CL increased, so resulting in a high thermal efficiency. While the SPMB has not only a long incomplete combustion flame length due to a lack of primary and secondary air not also it is still suppressed by a vessel bottom as increasing in CL that theirs cause a low thermal efficiency in the SPMB at a short of H. Table 4.4 shows the thermal efficiency of the CB and SPMB and the thermal efficiency contributions of them are shown in appendix D.

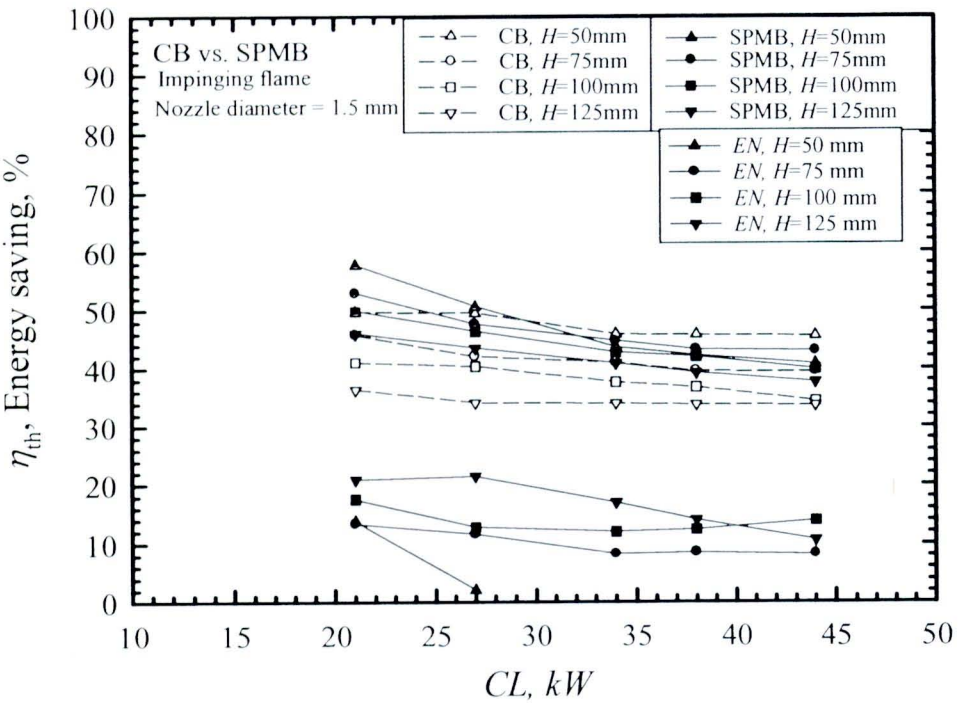

Figure 4.8 Thermal efficiency and energy saving of impinging flame.

The CB has a low thermal efficiency as compared with the SPMB because a main-flame characteristic of CB is an open combustion flame [6] so that it is only obtained by convective heat transfer. While the SPMB has a two modes of heat transfer that are convection mode from a long-post flame and radiation mode from matrix-stabilized flame within the packed bed that resulting in higher thermal efficiency than the CB. Thus the radiative heat transfer is a significant factor of thermal efficiency enhancement in the self-aspirating gas burner.

Table. 4.4 Thermal efficiency for the CB and SPMB.

CL, kW	η_{th} of the CB, %				η_{th} of the SPMB, %			
	H, mm				*H*, mm			
	50	75	100	125	50	75	100	125
21	49.70	45.80	41.05	36.41	57.64	52.88	49.79	46.03
27	49.51	42.05	40.38	34.11	50.59	47.57	46.31	43.44
34	45.89	40.97	37.60	33.93	43.55	44.63	42.73	40.85
38	45.70	39.51	36.75	33.73	42.13	43.17	41.94	39.24
44	45.58	39.42	34.36	33.64	40.72	42.92	39.91	37.63

Although an average of thermal efficiency of the SPMB is more than the CB but it is sacrificed by a high CO emission level (see in figure 4.3) because of a limitation of secondary air entrainment in the single flame at low H and low CL. From figure 4.8, a suitable condition for using the SPMB in the SMEs that is $CL \geq 34$ and $H = 125$ mm.

4.2.5 Energy saving

Energy saving (EN) for the SPMB with respect to the CB is calculated by Eq. (4.3) [6]. Basic of EN base on a same thermal output of each burner at same condition. Figure 4.8 shows the calculated EN of the SPMB as compared with the CB. At a constant H, EN decreases as the CL is increased because of a high heat loss to surrounding. But EN is increased by an increasing of H due to a low thermal efficiency of CB at high H. At $H =$ 50 mm and $CL > 27$ kW, the EN can not calculated because the thermal efficiency of the CB is higher than the SPMB. The maximum EN is 21.48% at the $CL = 27$ kW and H = 125 mm. A detail of EN is shown in table 4.5.

$$EN = \frac{(\eta_{SPMB} - \eta_{CB})}{\eta_{SPMB}} \times 100\% \qquad (4.3)$$

From the result, the SPMB has a high thermal efficiency that causes a high energy saving [60]. An average of η_{th} of the SPMB is higher than the CB about of 4.38%, yielding a relatively high of energy saving of about 9.80% in average over the operating range. Following the EN of the SPMB, we suggest to replace the CB in the SMEs of Thailand with the SPMB that will reduce cost of LPG consumption in Thailand about of 1,649 million baht/year (based on 2010) [10] that is not considered with economic costs.

Table. 4.5 Energy saving of the SPMB as compared with the CB.

CL, kW	EN, %			
	H, mm			
	50	75	100	125
21	13.76	13.39	17.56	20.91
27	2.14	11.59	12.80	21.48
34	-5.37*	8.16	12.02	16.95
38	-8.47*	8.48	12.38	14.05
44	-11.94*	8.16	13.91	10.59

*the η_{CB} is higher than the η_{SPMB}